[23a]

A. DI GERLANDO - I. VISTOLI

D.C. POLARIZED CURRENT TRANSFORMERS FOR THE MEASUREMENT OF HARMONIC NOISE: NUMERICAL AND EXPERIMENTAL ANALYSIS

ICHPS V - INTERNATIONAL CONFERENCE
ON HARMONICS IN POWER SYSTEMS

ATLANTA (GA USA), 22-25 SETTEMBRE 1992

ICHPS V

International Conference on Harmonics in Power Systems

September 22-25, 1992

Swissôtel
Atlanta, GA USA

Sponsored by:
IEEE Power Engineering Society

D.C. POLARIZED CURRENT TRANSFORMERS FOR THE MEASUREMENT OF HARMONIC NOISE: NUMERICAL AND EXPERIMENTAL ANALYSIS

Antonino Di Gerlando Ivo Vistoli

Dipartimento di Elettrotecnica, Politecnico di Milano
Piazza Leonardo da Vinci, 32 - 20133 Milano, Italy

Abstract - The paper describes the method employed for calculating the parameters of the model of a current transformer (C.T.) designed to detect the harmonic content of unidirectional currents generated by static convertors on their D.C. side. The paper also analyses the experimental results obtained during tests carried out on a prototype C.T., comparing them with the values calculated from the theoretical model.

INTRODUCTION

The detection of the harmonic content of unidirectional currents generated by static convertors presents considerable difficulties in certain cases, particularly when the harmonic current amplitudes are of the order of 10^{-3} to 10^{-4} times the D.C. component of the current.

During an earlier study [2] an algorithm has been developed for the design of a C.T. employing an air gap in its core. This device makes possible the measurement of harmonic currents only, and presents the double advantage of filtering out the D.C. and providing D.C. isolation between the measuring circuit and the power system. At the same time, it assures an acceptable ratio error over the frequency range $10 \div 10^4$ Hz. In [2] it is also described the development of a mathematical model for the evaluation of the ratio error over the entire frequency range mentioned. This model takes into account the influence of magnetic phenomena (eddy currents in laminations and secondary leakage inductance) as well as the effect of parasitic capacitances.

The present study considers the problem of calculating the design parameters of the C.T. model. Particular attention is given to the calculation of the equivalent parasitic capacitance, arriving at the determination of a simplified expression for calculating the main resonance frequency in high-frequency operation.

The paper shows many test results, obtained on a suitably constructed C.T. prototype. These consist of frequency response curves (at different A.C. and D.C. current amplitudes), examples of transformation of some waveforms and curves showing the transient response to a step input. These results, compared with those obtained by numerical simulation, confirm the quality of the model adopted and of the method used for calculating its parameters. The results also yield further informations in guiding and improving the design.

CALCULATION OF PARAMETERS

The lumped-parameter electrical model adopted for the study of the C.T. operation is the well-known T-type equivalent circuit.

Given the width of the band covered ($10 \div 10^4$ Hz), the parameters cannot be considered as constant. This applies particularly to the derived branch parameters (G_o, L_o), which are sensitive to the influence of eddy currents.

As for the distributed capacitances of the windings, which affect the performance at high frequencies, an approximate representation is possible, enabling the calculation of the first resonance frequency. This consists of representing the overall capacitance effect by means of a single equivalent parasitic capacitance C, placed immediately after the ideal transformer [2, 3].

Estimating the equivalent parasitic capacitance

A possible evaluation criterion is based on the formulation of an energy-type equivalence between the total dielectric energy distributed among the network of single parasitic capacitances and the energy pertaining to the capacitance C in the equivalent circuit.

For this purpose, the expression for the dielectric energy distributed in the secondary winding is formulated with reference to a working situation in which it can be claimed that the inter-turn capacitances do not substantially affect the voltage distribution between the winding turns, due to the induced e.m.f.s and to the voltage drops. This assumption, which is perfectly acceptable in low and medium-frequency operation, leads to the evaluation of the total equivalent capacitance C. This value of capacitance is also considered valid for the determination of the first resonance frequency.

It is clear that this representation, employing a single capacitance, does not permit the calculation of further resonance phenomena, which can be observed experimentally at even higher frequencies. On the other hand, it is the identification of the first resonance frequency which is the factor of major interest, insofar as it determines the upper limit of the acceptable range of operation for the C.T..

The basic element, on which the calculation is founded, is the capacitance per unit length between adjacent turns. This parameter can be estimated by using the expression for calculating the capacitance between the two parallel conductors of a bifilar line. If "dc" denotes the diameter of the metallic wire and "h" the distance between the axes of the wires, the capacitance per unit length C' is given by:

$$C' = \frac{\pi \cdot \varepsilon_r \cdot \varepsilon_o}{\ln(2 \cdot h/dc - 1)} \quad [F/m] \quad . \qquad (1)$$

Eq.(1) is exact when the distance h is large compared with the diameter dc. As a first approximation, however, it is assumed to be valid also in the case being examined. In addition, the dielectric constant ε_r which appears in eq.(1) is taken as a suitable value between those for air and for the insulant, depending upon the distance h between the wires.

Thus, the capacitance between two adjacent turns, calculated on the basis of the average length ℓ_{mz} of a turn in the secondary winding, is:

$$C_t = C' \cdot \ell_{mz} \quad . \qquad (2)$$

The secondary winding, containing N_z turns, is constructed using a number of superimposed layers of adjacent turns. Fig.1 shows the structure of the network of distributed capacitances corresponding to this type of winding. The example shown in the figure refers to a winding of 4 layers, which are wound and superimposed in accordance with the numerical sequence shown there.

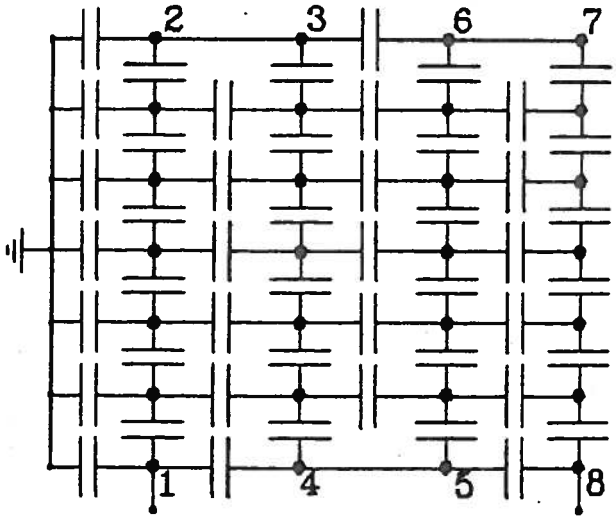

Fig. 1. Network of capacitances between turns and to mass, for a four-layer wire winding.

The capacitances appearing in the network of fig.1 can be divided into three categories, as follows:
- capacitances between adjacent turns in the same layer (vertical capacitances);
- capacitances between the turns of the first layer (lying between the extreme turns indicated with 1 and 2) and the core mass (horizontal capacitances connected to the earth symbol);
- capacitances between adjacent turns in different layers (remaining horizontal capacitances).

If it is assumed that the distances between the turns are all equal, it can be concluded that all the capacitances between turns have the same value (C_1). At the same time, applying the "image principle" to the equipotential metallic surface of the core, one can deduce that capacitances to earth are also C_1 each. On the other hand, an imperfect determination of the latter capacitances does not significally affect the total distributed dielectric energy, as their additional contribution is small.

Let us refer to a generic winding, made up of N turns arranged in m adjacent and alternating layers and let a voltage V be applied to its terminals. Continuing with the assumption that the voltages between the turns are not modified by the presence of interturn capacitances, it can be stated that:
- all the vertical capacitances are subjected to the same voltage, equal to the voltage per turn (V/N);
- the capacitances to earth are subjected to half the above voltage;
- the capacitances between turns in different layers are subjected to different voltages, depending on whether the adjacent wires are electrically close or distant.

If V_k indicates the generic voltage across the terminals of each single capacitance, energy equivalence is established by equating the sum of dielectric energies of all the capacitors in the network of fig.1 to the energy accumulated in a single equivalent capacitance C subjected to voltage V:

$$W_e = \frac{1}{2}\cdot C\cdot V^2 = \Sigma_k \frac{1}{2}\cdot C_1\cdot V_k^2 \quad . \qquad (3)$$

By applying eq.(3), one obtains the following general expression for the equivalent capacitance C, referred to the capacitance between adjacent turns C_1:

$$\frac{C}{C_1} = \frac{1}{4\cdot m\cdot N} + \frac{1}{N} + \frac{2}{3}\cdot\frac{m-1}{m}\cdot\left(\frac{1}{N}+\frac{1}{m}\right)\cdot\left(\frac{2\cdot N}{m}+1\right) \quad . \qquad (4)$$

The first term of the above expression represents the contribution corresponding to the capacitance to ground. It can be seen that it is a small quantity compared with the other terms. It should be noted that eq.(4) is also valid in the limit case of a single layer (m = 1), when the third term disappears.

By observing Tab.I, which gives the values of the ratio C/C_1, one can deduce that the equivalent capacitance increases with the number of turns in the winding (N). At a constant number N of turns, this capacitance decreases with the increase in the number of layers m. This result can be arrived at intuitively, considering that the capacitances between turns belonging to different layers are subjected to voltages proportional to the maximum voltage between layers (V/m), which decreases with an increase in m.

Tab.I - Values of the ratio C/C_1, as a function of the number of turns (N) and layers (m).

m \ N	20	30	50	100	1000	5000
2	3.9	5.5	8.9	17.2	167	834
3	2.5	3.5	5.4	10.3	99	494
4	1.7	2.3	3.5	6.6	63	313
6	-	1.3	1.9	3.4	31	155
10	-	-	0.8	1.4	12	60

It can thus be concluded that, in order to limit the value of the parasitic capacitance, the most suitable arrangement of the winding is that employing many alternating and superimposed layers.

Finally, it is justified to consider only the equivalent capacitance of the secondary winding in the equivalent circuit of the C.T., neglecting that of the primary winding. The very small number of primary turns ($N_1 < 10$, m = 1) makes capacitance effects between primary turns negligible. In other words the capacitance currents, flowing between adjacent turns of the primary, form an extremely small part of the current I_1.

The generic configuration shown in fig.1 refers to a situation in which a part of the ideal core, assumed to be rectilinear, is wound with a single winding consisting of identical, alternating layers. It is interesting to examine how the expression for calculating the equivalent capacitance becomes modified in the case in which explicit mention is made of a toroidal core (or a double C, which is equivalent to it).
Two different ways of arranging the secondary winding around the core can be considered:
- the first procedure consists of winding the turns around an already assembled core. In this way, successive layers are wound in the same sense, because of which this arrangement can be called "continuous winding with layers in the same sense". This type of construction is rather laborious (we talk of a so-called "knitted" winding). However, it is the only possible approach in the case of compact toroidal cores. It has the added advantage of producing a winding with a perfectly uniform distribution around the core, which yields considerable functional advantages;
- a different approach to the construction of the winding consists of winding the two half-cores separately, only then assembling the two halves. In this case, we have two equal coils, constructed using alternating layers, which are then connected in series. This type of winding, which is easier to make, can be called a "winding with coils using layers in the opposite sense".

In order to calculate the equivalent capacitance, a problem common to both the above winding types is the evaluation of the number of layers m making up the winding. It must be recognized that successive layers are made up of different numbers of turns, in that the turns

themselves are arranged on circumferences with diameters gradually decreasing towards the centre. It is possible to estimate the number of layers m in a winding of N turns wound upon a toroidal core using the following expression [4]:

$$m \approx \frac{n_{1s} + 3 - \sqrt{(n_{1s} + 3)^2 - 12 \cdot N}}{6} \quad , \qquad (5)$$

where n_{1s}, equal to the number of turns in the first layer wound around the core, is given by:

$$n_{1s} \approx \pi \cdot (D_n/h - 1) \quad , \qquad (6)$$

where h is still the distance between adjacent turns.

Let start to calculate the equivalent capacitance in the case of a continuous winding with layers in the same sense. Noting that the voltage between adjacent turns is V/N, while that between adjacent turns in different layers is still, in this case, V/m, the criterion of energy equivalence described by the eq.(3) leads to the following:

$$\frac{C}{C_t} = \frac{1}{N} \cdot \left(1 + \frac{1}{4 \cdot m}\right) + \frac{m - 1}{m^3} \cdot N \quad . \qquad (7)$$

It can be noted that the second term of eq.(7) easily dominates the first one, as soon as a significant number of turns and layers is considered. Apart from that, the comparison of values obtained from eq.(7) with those given by eq.(4) shows that the arrangement considered here is characterized by a lower value of equivalent capacitance.

The calculation of the ratio C/C_t in the case of the winding employing opposed-sense layers can be carried out easily, as it can be reduced to the case of an alternating-layer winding. The difference is that here we have two equal half-windings, of N/2 turn each, each of which is subjected to an overall voltage of V/2 (series connection).
Because of this, once the capacitance C^* of each half-winding is calculated using equation (4), the equivalent capacitance of the two coils in series becomes $C = C^*/2$. The following expression can now be derived:

$$\frac{C}{C_t} = \frac{1}{N} \cdot \left(1 + \frac{1}{4 \cdot m}\right) + \frac{1}{3} \cdot \frac{m - 1}{m} \cdot \left(\frac{2}{N} + \frac{1}{m}\right) \cdot \left(\frac{N}{m} + 1\right) \quad , \qquad (8)$$

where N is the total number of turns of two coils in series and m is the number of layers in each of them.
In eq.(8), too, the first term becomes negligible in comparison with the second once the number of turns and layers grows beyond a very small figure. It can also be seen that the values obtained fron eq.(8) are about 1/3 of those calculated from eq.(7), other things being equal. It thus appears that the arrangement using opposed-layer coils is advantageous compared with the alternative one.

Dependence of the resonance frequency on the construction and winding data of the C.T.

On the basis of the relations obtained, it is possible to reach an expression for estimating the resonance angular frequency ω_{res} of the C.T. secondary winding. The respective expression is [2]:

$$\omega_{res} = \frac{1}{\sqrt{L_2 \cdot C}} \cdot \sqrt{1 - \frac{R_{2t}^2 \cdot C}{L_2}} \approx \frac{1}{\sqrt{L_2 \cdot C}} \quad , \qquad (9)$$

where R_{2t} is the sum of the internal secondary resistance R_2 and of the measuring resistance R_m.
Referring to the opposed-layer winding, by assuming that $N_2 \gg m \gg 1$, eq.(8) can be reduced to the following:

$$\frac{C}{C_t} \approx \frac{1}{3} \cdot \frac{m - 1}{m^3} \cdot N_2 \quad ; \qquad (10)$$

on the other hand, putting eq.s (1) and (2) together, we can write:

$$C_t = \nu_c \cdot \pi \cdot \varepsilon_r \cdot \varepsilon_o \cdot \ell_{m2} \quad , \qquad (11)$$

where ν_c, called proximity factor, is a coefficient depending on the closeness between the conductors, and equals:

$$\nu_c = \frac{1}{\ln(2 \cdot h/d_c - 1)} \quad . \qquad (12)$$

Because of this, the equivalent capacitance of a winding employing two coils is:

$$C \approx \nu_c \cdot \pi \cdot \varepsilon_r \cdot \varepsilon_o \cdot \frac{m - 1}{3 \cdot m^3} \cdot \ell_{m2} \cdot N_2 \quad . \qquad (13)$$

As far as the leakage inductance L_2 of the secondary winding is concerned, the total value equals twice the inductance L_c of each coil, made up of $N_2/2$ turns. Attributing to the secondary winding, as an approximation, only the entire leakage flux which passes it in the longitudinal direction, we can put down the following:

$$L_2 = 2 \cdot L_c \approx 2 \cdot \left(\frac{N_2}{2}\right)^2 \cdot \mu_o \cdot \frac{\ell_{m2} \cdot a_2}{3 \cdot h_a} \quad , \qquad (14)$$

where a_2 is the thickness of the secondary winding and h_a the height of the windings of each coil pair.
On the other hand, it is easy to show that:

$$a_2/h_a = m \cdot (m - 1)/N_2 \quad ; \qquad (15)$$

from which we obtain:

$$L_2 \approx \frac{1}{6} \cdot \mu_o \cdot m \cdot (m-1) \cdot \ell_{m2} \cdot N_2 \quad . \qquad (16)$$

Eq.(9) for the resonance angular frequency ω_{res} becomes accordingly (for $m > 1$):

$$\omega_{res} \approx \sqrt{\frac{18}{\pi \cdot \mu_o \cdot \varepsilon_r \cdot \varepsilon_o \cdot \nu_c}} \cdot \frac{m}{m - 1} \cdot \frac{1}{\ell_{m2} \cdot N_2} \quad . \qquad (17)$$

The analysis of eq.(17) allows us to draw the following conclusions, of importance in the design:
- insulation conditions between conductors have an influence, albeit a minor one, on the resonance frequency. The more tightly the conductors are packed (high values of ν_c), the lower the value of ω_{res}. The same result is obtained when using insulants with a higher dielectric constant ε_r;
- if the number of layers m is rather high, its influence on the resonance frequency is negligible;
- the higher the average length of turns ℓ_{m2}, the lower the resonance angular frequency ω_{res}; because of this, the resonance frequency is inversely proportional to the dimensions of the device;
- the higher the number of secondary turns N_2, the lower the resonance frequency.

In conclusion, it can be stated that, whilst the increase in the product $N_2 \cdot D_n^2$ permits the lowering of the lower cut-off frequency of the C.T. passband [2], this choice is also followed by a reduction in the resonance frequency and, accordingly, in the higher limit of the useful band of the transformer.

Eq.(17) can thus be employed at the design stage to determine the limiting values for the dimensions and the number of secondary turns of the C.T., so that these satisfy the specified level of accuracy in the transformation ratio over the frequency band requested.

NUMERICAL SIMULATION AND EXPERIMENTAL ANALYSIS

A suitably constructed prototype [2] has been subjected to some experimental tests, together with numerical simulations, in order to check the soundness of the design methods and of the model for the study of the operation of the gapped C.T..

Bearing in mind that the primary current A.C. components (I_1) are very small compared with the direct current I_{dc}, it has been considered convenient to construct the primary winding of the prototype using two metallically separate conductors. The conductor with the larger

cross-section forms a path for the D.C., while the conductor with the smaller cross-section, wound together with the preceding one, forms a path for the A.C. component. In this way, the amplitude of these two components can be controlled and measured more conveniently.

Influence of the amplitude of the A.C. and D.C. components.

The first quantity to be checked is the error sensitivity of the C.T. ratio as the amplitudes of the D.C. and A.C. components vary over the frequency band of interest (about 1 to 10^4 Hz). Tab.II shows measured values of the ratio I_R/I_{1s} (I_R being the current in the measuring resistance R_m = 10 kΩ and I_{1s} the primary current referred to the secondary) as the frequency is varied, at two different values of the D.C. current I_{dc} and of the A.C. current I_1.

Tab.II - Sensitivity of the current ratio I_R/I_{1s} to the amplitude of the D.C. (I_{dc}) and A.C. (I_1) primary components, as a function of the frequency (measured values).

f [Hz]	10	100	1000	10000
I_R/I_{1s} (I_{dc}=0 A; I_1=5 mA)	0.9198	0.9779	0.9908	1.0265
I_R/I_{1s} (I_{dc}=20 A; I_1=5 mA)	0.9073	0.9715	0.9906	1.0245
I_R/I_{1s} (I_{dc}=0 A; I_1=40 mA)	0.9204	0.9778	0.9906	1.0265
I_R/I_{1s} (I_{dc}=20 A; I_1=40 mA)	0.9147	0.9754	0.9904	1.0245

The values in Tab.II show that the current ratio has a certain dependance on the frequency of the current I_1 considered. The error at low frequency is shown to be higher than the value predicted at the design stage (5%). This deviation can be attributed partly to the uncertainty as to effective value of the geometrical gap and partly to the deterioration of the magnetic characteristics of the laminations following the mechanical processes undergone during the construction of the core.

Examining the different values of the ratio at any particular frequency, it can be seen that, whilst the influence of the amplitudes of the primary components, both D.C. and A.C., is not zero, it is very small indeed. This confirms the correctness of having chosen, at the design stage [2], a low value (about 0.12) for the core magnetic factor λ_n:

$$\lambda_n = \frac{\ell_n / 2}{(\mu_{rev}/\mu_0)\cdot\delta} ,$$

which is equal to the ratio between the magnetic half-length of the core and the geometrical air gap. In this way, the influence of the core, which is due to the variation of the reversible permeability μ_{rev} with load [1, 5], is much reduced.

Frequency response

The numerical and experimental study of the frequency response of the C.T. prototype, connected to a measuring resistance R_m = 10 kΩ, has given the results shown in fig.2. The measured points are connected with a broken line, while those obtained from computer simulation are joined with a solid line.

The calculated parameters of the C.T. equivalent circuit, adopted for the simulation (values referred to the secondary) are as follows:

- values of the derived branch parameters (at 400 Hz):
  $L_0 \approx 420$ H; $R_0 \approx 1$ MΩ;
- secondary leakage inductance and resistance:
  $L_2 \approx 0.23$ H; $R_2 \approx 700$ Ω;
- secondary winding equivalent capacitance: C ≈ 67 pF.

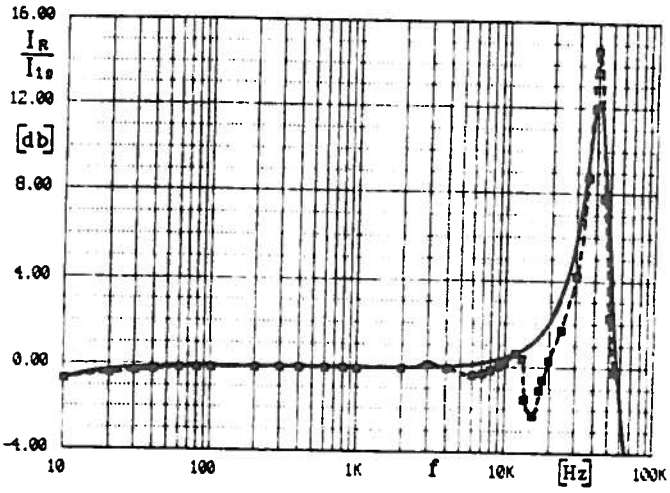

Fig. 2. Frequency response of the C.T. prototype; measured: ----▪---- ; calculated: ——— ; R_m = 10 kΩ .

On the basis of these values, the calculation [2] of the principal resonance frequency and of the current ratio under resonant conditions gives the following results:

$\omega_{res} \approx 40.5$ kHz; I_R/I_{1s} [db] $\approx 20\cdot\log_{10}(5.86) = 15.4$.

It can be seen that a good agreement exists between the above values and the measured ones shown in fig.2. The discrepancies between calculated and measured results, which can be noticed around 15 kHz, are due to further resonance phenomena, probably because of distributed effects of the parasitic capacitances.

Fig.3 shows a numerical and experimental analysis conducted on the same C.T. prototype, but with the secondary connected to a measuring resistance R_m = 100 Ω.

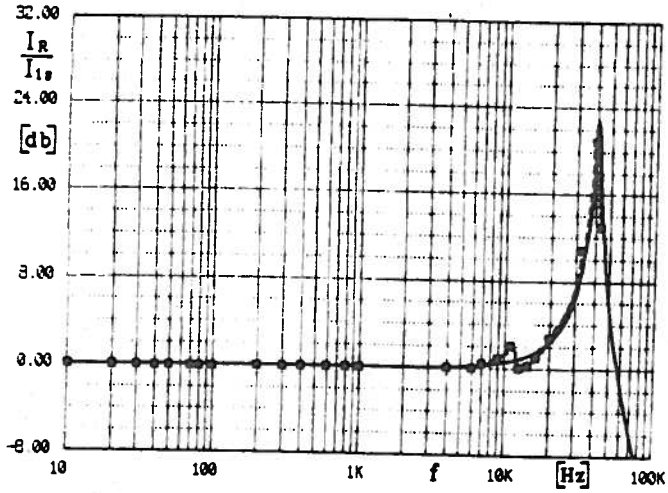

Fig. 3. As in fig.2, except that R_m = 100 Ω.

It can be seen that the ratio error at low and medium frequencies is negligible, compared with that of the preceding case. The resonance frequency remains practically unchanged (according to eq.(9), it depends mainly on L_2 and C), while the magnitude of the ratio near the resonance frequency is significantly higher.
The behaviour of the transformer over the frequency range of interest (up to 10 kHz) appears better than in the case of R_m = 10 kΩ. It is, however, clear that the use of a measuring resistance R_m = 100 Ω means that the signal measured across the secondary is equal to one hundredth of that in the case of R_m = 10 kΩ, thus calling for the use of an amplifier.

Examples of transduced waveforms

Some experimental oscillograms, obtained with a digital oscilloscope, are shown below. What is being measured is the reproduction on the secondary side of certain current waveforms imposed upon the primary.

In all the oscillograms the upper signal is the voltage across a measuring resistance of 10 Ω connected in series with the primary ($N_1 = 5$). The lower signal is the voltage across the resistance $R_m = 10$ kΩ connected to the terminals of the secondary winding ($N_2 = 8000$).

Tests using a sinusoidal waveform (not shown here for the sake of brevity) have demonstrated that this waveform is reproduced, without any distortion, over the entire frequency range.

Fig.4 shows the reproduction of triangular and rectangular waveforms, at a frequency of 10 Hz. The very low value of this frequency justifies the distortion visible on the secondary side, which is particularly pronounced in the case of rectangular waveform.

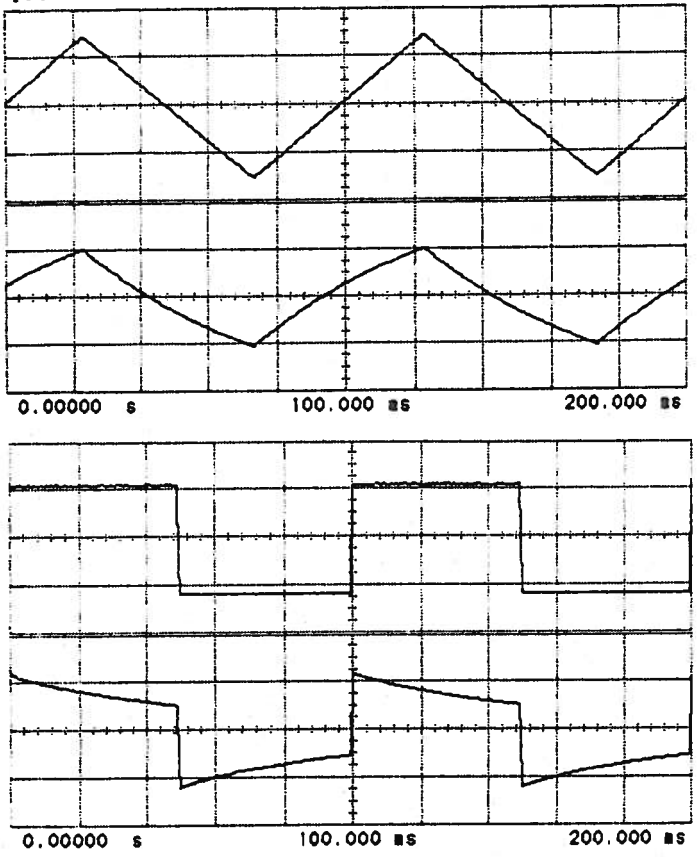

Fig. 4. Experimental reproduction of triangular and rectangular waveforms at 10 Hz;
scales: upper = 500 mV/d; lower = 400 mV/d.

In addition, referring to the case of the rectangular waveform, the step variations in primary current give rise to a sequence of RL type transients (where R = R_o, L = L_o), with exponential segments.

It has been observed that, at a frequency of 50 Hz, the triangular waveform is reproduced in a substantially correct manner, while the rectangular one, in spite of a considerable improvement, still exhibits a certain degree of distorsion.

Figure 5.a shows that, at a frequency of 100 Hz, the rectangular waveform as reproduced on the secondary side is practically free of exponential decay. At frequencies higher than 200 Hz, during the time intervals immediately following each inversion of the square waveform, high-frequency transient oscillations are present (see fig.5.b, where f = 500 Hz). The origin of this oscillations is linked to the fact that, under those conditions, the device is equivalent to a second-order electrical circuit, made up of two parallel branches: the equivalent capacitance C and the branch consisting of R_{z1} and L_z connected in series.

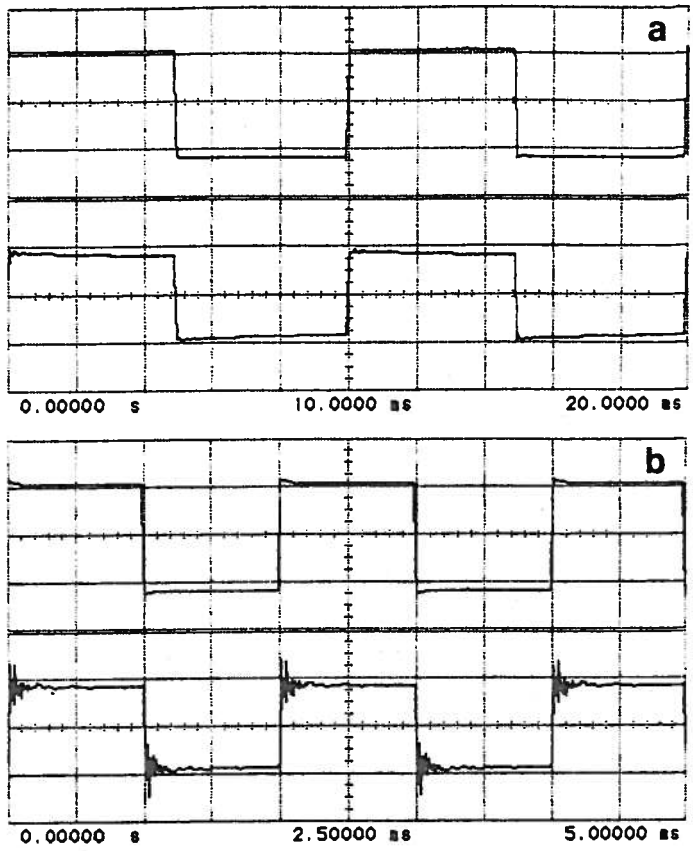

Fig. 5. Experimental reproduction of rectangular waveforms: (a) = 100 Hz; (b) = 500 Hz;
scales: upper = 500 mV/d; lower = 400 mV/d.

The study of this RLC circuit using state equations leads to the calculation of the natural complex frequency $\lambda_r \mp j\cdot\lambda_i$, which is given by:

$$\lambda_r \mp j\cdot\lambda_i = \frac{R_{z1}}{2\cdot L_z} \mp j\cdot\frac{1}{\sqrt{L_z\cdot C}}\cdot\sqrt{1-\frac{R_{z1}^2\cdot C}{L_z}} \qquad (18)$$

On the basis of the numerical value of the parameters, it can be recognised that the angular frequency λ_i of the oscillation coincides in practice with the resonance angular frequency ω_{res}.

Figure 6 shows an experimental oscillogram of the step response of the C.T. prototype.

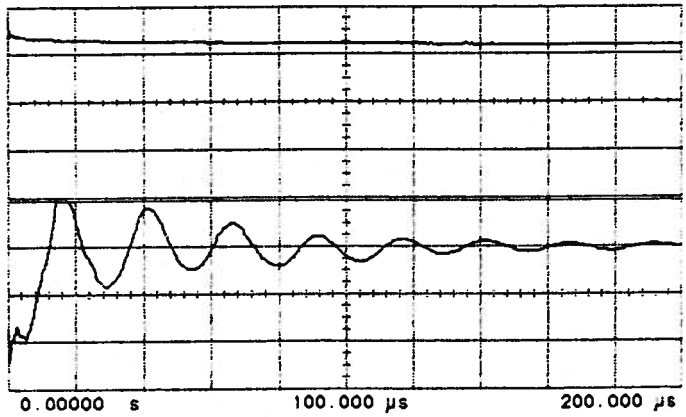

Fig. 6 Experimental step response of the C.T.: scales: upper = .5 V/d; lower = .4 V/d; time = 20 µs/d.

The natural frequency of oscillation in fig.6 equals about 40 kHz, which agrees very well with what has been deduced from the frequency response in figures 2 and 3.

As for the reproduction of the triangular waveform, the behaviour of the C.T. remains acceptable for frequencies up to about 2 kHz. At higher frequencies, appreciable distortion phenomena appear (see fig. 7).

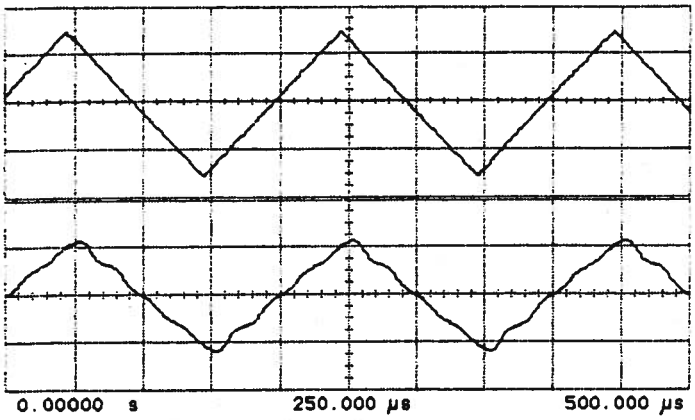

Fig.7. Experim. reproduction of a triangular waveform at 5 kHz; scales: upper = .5 V/d; lower = .4 V/d.

In this case too, these are attributable to the effects caused by parasitic capacitances at high frequencies.

Overall, the results shown demonstrate that the C.T. prototype is behaving satisfactorily.

Sensitivity of the C.T. response to the variation of parameters

The results of some simulations carried out by varying the parameters of the C.T. equivalent circuit are shown in the following. The model adopted uses, for simplicity, constant values for the parameters of the derived branch, without considering their frequency dependence as a first approximation.

a) Magnetizing inductance

Fig.8.a and 8.b show the effect of an increase in the magnetizing inductance on the frequency response and on the step response respectively.

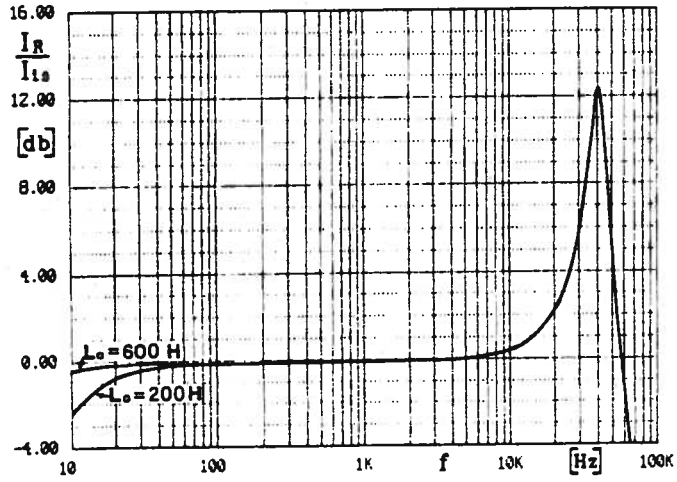

Fig.8.a. Sensitivity of the C.T. to the variation of the magnetizing inductance: frequency response.

When the value of inductance Lo is increased from 200 H (see the lower curve in fig.8a) to 600 H (curves further above), the low-frequency ratio improves, while the C.T. behaviour at higher frequencies remains unchanged. In the time domain (fig.8b), the initial transient oscillation is unchanged, while the slope of the exponentially decreasing segment becomes smaller.

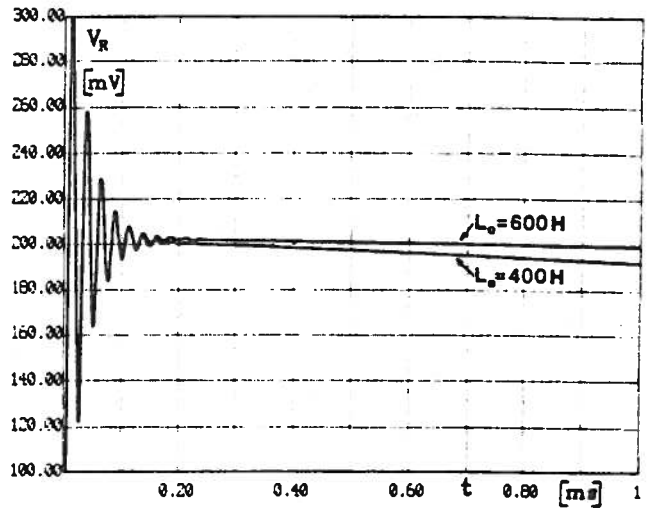

Fig.8.b. Sensitivity of the C.T. to the variation of the magnetizing inductance: step response.

b) Core losses equivalent resistance

A lower value of the resistance Ro (corresponding to the adoption of a more dissipative magnetic material) gives rise to a lower frequency response, over the entire frequency band.

The effect of higher loss in the magnetic material can be seen very well in the step response (see fig.9).

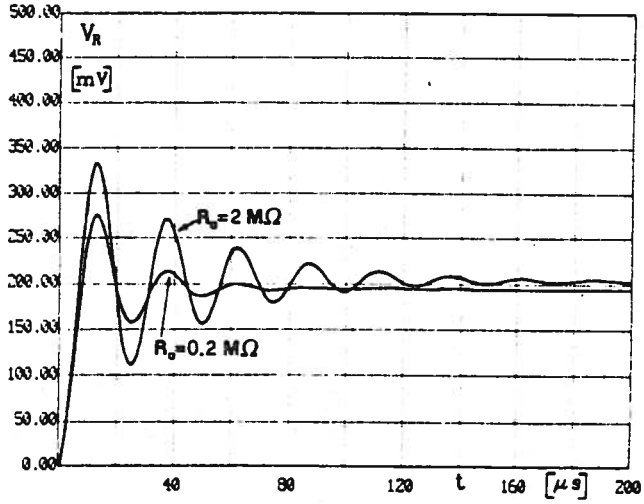

Fig. 9. Sensitivity of the C.T. to the variation of the core losses equivalent resistance: step response

The variation in Ro has a small influence only on the natural resonance frequency, while it strongly affects the exponential decrement in the envelope of the oscillation, which is more pronounced as Ro decreases.

c) Secondary winding equivalent capacitance

It can be seen from fig. 10 that a reduction in the equivalent capacitance of the secondary shifts the resonance frequency to higher values of frequency, while at the same time increasing the peak value at resonance. It can be correspondingly showed that, for lower values of capacitance, the oscillation forming part of the step response has a higher natural frequency, accompanied by a lower amplitude and duration.

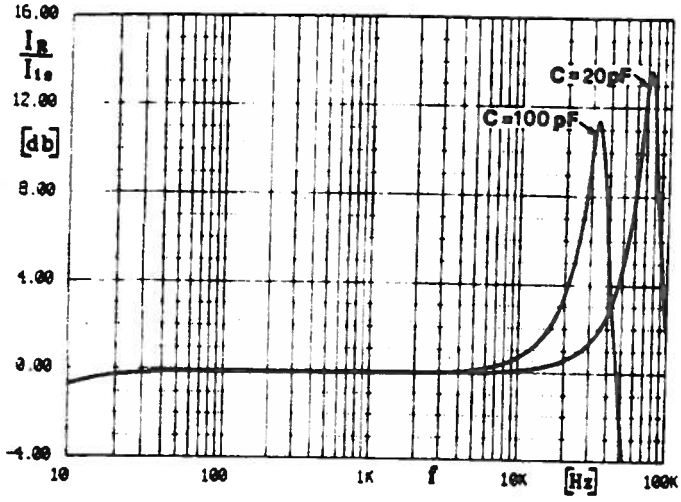

Fig.10. Sensitivity of the C.T. to the variation of the equiv. secondary capacitance: frequency response

d) Secondary leakage inductance

Lower values of the secondary leakage inductance shift the resonance frequency towards higher values, accompanied by lower peak amplitudes. The step response (see fig.11) is improved, in terms of a reduction in both the amplitude of the oscillation and in its duration.

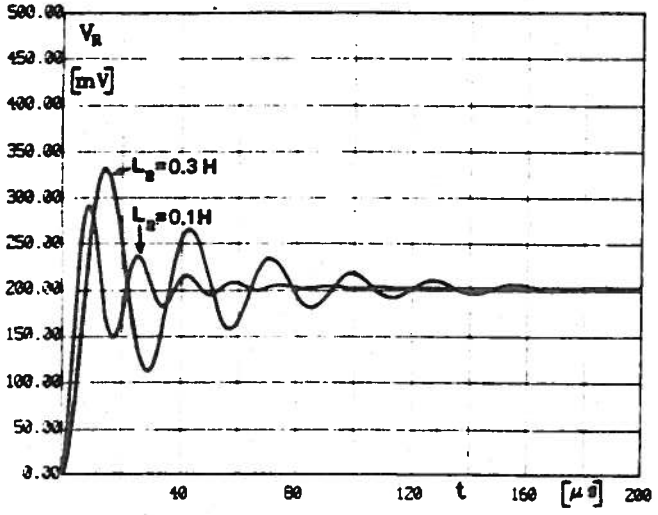

Fig.11. Sensitivity of the C.T. to the variation of the secondary leakage inductance: step response.

e) Measuring resistance

A reduction in the measuring resistance R_m produces an improvement in the frequency response at its lower end (see fig.12.a). This reduction has practically no effect on the frequency of the resonance, but produces an increase in its peak amplitude.

In terms of the step response (see fig.12.b), lower values of R_m produce higher amplitudes and durations of oscillations (as the system is less dissipative), while their natural frequency remains unchanged.

CONCLUSIONS

The work described consists of the study of a current transformer designed to detect the harmonic content of a D.C. current, whose intensity is much higher than that of A.C. harmonic components. The latter are contained in a frequency band extending from 10 to 10^4 Hz.

Particular attention has been given to the calculation of the equivalent value of the distributed capacitance of the windings and to estimating the main resonance frequency in the frequency response of the device.

A first prototype of this current transducer has been built and tested. Its performance features give satisfactory precision, while the characteristics are basically in accordance with the theoretical design study and with computer simulation.

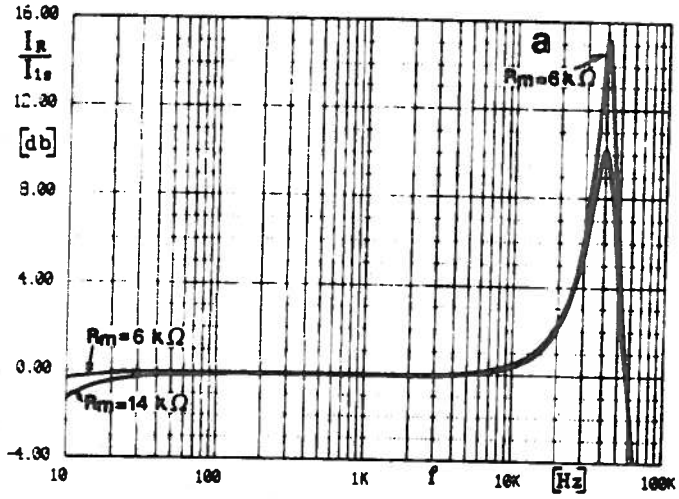

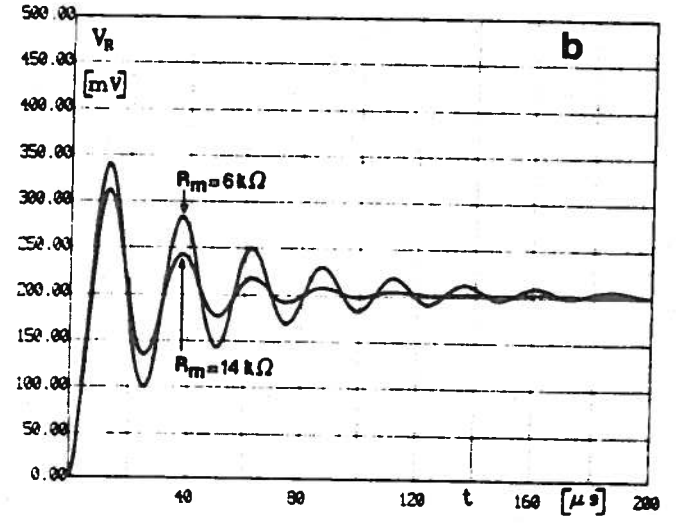

Fig.12. Sensitivity of the C.T. to the variation of the meas. resistance: frequency and step responses.

REFERENCES

[1] A. Di Gerlando, I. Vistoli: "Special Transformers for the Measurement of Harmonic Noise of D.C. Currents"; Symposium "SPEEDAM", 19-21 May 1992, Positano, Italy.

[2] A. Di Gerlando, I. Vistoli: "D.C. polarized Current Transformers for the Measurement of Harmonic Noise: Design and Modelling Methodologies"; ICHPS V Conference, Atlanta, Georgia, USA, September 23-25, 1992.

[3] D. A. Douglass: "Current Transformer Accuracy with asymmetric and high Frequency fault Currents"; IEEE Trans. on P.A.S., Vol. PAS-100, N°3, March 1981.

[4] E. London: "Practical Transformer Design Handbook"; Tab Books Inc., Blue Ridge Summit, PA, 1989.

[5] R. Bozorth: "Ferromagnetism"; D. Van Nostrand, New York, 1951.